

Priming and filtering of antiherbivore defences among *Nicotiana attenuata* plants connected by mycorrhizal networks

Yuanyuan Song^{1,2} | Ming Wang¹ | Rensen Zeng²  | Karin Groten¹ | Ian T. Baldwin¹ 

¹Department of Molecular Ecology, Max Planck Institute for Chemical Ecology, Jena 07745, Germany

²Key Laboratory of Ministry of Education for Genetics, Breeding and Multiple Utilization of Crops, College of Crop Science, Fujian Agriculture and Forestry University, Fuzhou 350002, China

Correspondence

Ming Wang and Ian T. Baldwin, Department of Molecular Ecology, Max Planck Institute for Chemical Ecology, Hans-Knöll-Str. 8, Jena 07745, Germany.
Email: mawang@ice.mpg.de; baldwin@ice.mpg.de

Funding information

Max Planck Society; European Research Council Advanced Grant ClockworkGreen, Grant/Award Number: 293926; National Natural Science Foundation of China, Grant/Award Numbers: 31770474 and 31670414; China Scholarship Council, Grant/Award Number: 201608350018

Abstract

Arbuscular mycorrhizal fungi (AMF) establish symbiotic associations with a majority of terrestrial plants to form underground common mycorrhizal networks (CMNs) that connect neighbouring plants. Because *Nicotiana attenuata* plants do not respond to herbivory-elicited volatiles from neighbours, we used this ecological model system to evaluate if CMNs function in interplant transmission of herbivory-elicited responses. A mesocosm system was designed to establish and remove CMNs linking *N. attenuata* plants to examine the herbivory-elicited metabolic and hormone responses in CMNs-connected “receiver” plants after the elicitation of “donor” plants by wounding (W) treated with *Manduca sexta* larval oral secretions (OS). AMF colonization increased constitutive jasmonate (JA and JA-Ile) levels in *N. attenuata* roots but did not affect well-characterized JAs-regulated defensive metabolites in systemic leaves. Interestingly, larger JAs bursts, and higher levels of several amino acids and particular sectors of hydroxygeranylinalool diterpene glycoside metabolism were elevated in the leaves of W + OS-elicited “receivers” with CMN connections with “donors” that had been W + OS-elicited 6 hr previously. Our results demonstrate that AMF colonization alone does not enhance systemic defence responses but that sectors of systemic responses in leaves can be primed by CMNs, suggesting that CMNs can transmit and even filter defence signalling among connected plants.

KEYWORDS

defence priming, mycorrhizal network, *Nicotiana attenuata*, *Rhizophagus irregularis*, signal filtering

1 | INTRODUCTION

More than 80% of terrestrial plant species, including most agriculturally important crops, can form symbiotic associations with arbuscular mycorrhizal fungi (AMF) from the phylum Glomeromycota (Brundrett & Tedersoo, 2018; Martin, Uroz, & Barker, 2017; Schussler, Schwarzott, & Walker, 2001). Fossil records and phylogenetic research have dated this most widespread of plant symbioses to 450 million years ago, to a time when green plants began to colonize the earth

(Smith & Read, 2010), suggesting a key role of mycorrhizae in facilitating terrestrialization. Intracellular fungal structures penetrate root cortical cells and form arbuscules where the all-important exchange of nutrients between plant and fungus occurs (Luginbuehl & Oldroyd, 2017). It is mainly in the arbuscule where a plant trades reduced carbon from photosynthesis for phosphorous (P) and nitrogen (N) supplied by the fungus (Cruz et al., 2007; Ezawa, Smith, & Smith, 2002; Govindarajulu et al., 2005; Hijikata et al., 2010; Javot, Penmetsa, Terzaghi, Cook, & Harrison, 2007; Tanaka & Yano, 2005). The effects of mycorrhizal associations can be seen beyond the plant and into the rhizosphere, where mycorrhizae alter carbon deposition, soil structure,

Yuanyuan Song and Ming Wang contributed equally to this work.

and microbial diversity, which are thought to indirectly influence the outcome of plant interactions with other organisms (Cavagnaro, Bender, Asghari, & van der Heijden, 2015; Smith & Read, 2010). Furthermore, mycorrhizal extraradical hyphae are able to colonize roots of different plant individuals and species to form underground common mycorrhizal networks (CMNs), which link multiple plants growing together in communities. The lack of specificity in the interactions between plants and fungi in mycorrhizal symbioses allows plants to associate with each other via CMNs, perhaps to establish cooperative guilds (Perry, 1995). CMNs are thought to play vital roles in plant establishment, resource allocation, species diversity, succession within plant communities, and ecosystem stability (Selosse, Richard, He, & Simard, 2006; Simard et al., 2012; Van Der Heijden & Horton, 2009), and hence, understanding the ecological functions of CMNs may provide novel approaches for ecosystem management.

The consequences of AMF colonization for host plants are far ranging and are generally classified by two outcomes: growth promotion and resistance enhancement. Evidence of enhanced plant resistance by AMF against abiotic stresses such as drought, salinity, osmotic imbalances, heavy metal, or heat are perhaps the best described (Chitarra et al., 2016; Giri, Kapoor, & Mukerji, 2003; Johnson, Graham, & Smith, 1997; Lenoir, Fontaine, & Sahraoui, 2016; Hildebrandt, Regvar, & Bothe, 2007; Rodriguez et al., 2008). AMF symbioses are also thought to provide enhanced resistance/tolerance of plants against biotic stresses such as pests, pathogens and parasitic plants (Cameron, Neal, van Wees, & Ton, 2013; Pineda, Zheng, Van Loon, Pieterse, & Dicke, 2010). In AMF-colonized roots, the accumulation of certain defence compounds (e.g., phenolics and defence-mediating hormones) and reactive oxygen species have been reported (Laparré et al., 2014; MacLean, Bravo, & Harrison, 2017). Amelioration of the adverse effects of infestation by endoparasitic nematodes (Elsen, Gervacio, Swennen, & De Waele, 2008; Vos et al., 2012) and root herbivores has also been reported, such as the dramatic 50% reductions in larval mass gain and survival of the black vine weevil (*Otiorhynchus sulcatus*) on AMF-colonized strawberry roots (Gange, 2001; Gange, Brown, & Sinclair, 1994). However, other studies have failed to find AMF-associated increases in resistance, such as with the clover root weevil larvae (*Sitona lepidus*) whose growth was independent of AMF inoculation (Currie, Murray, & Gange, 2011). AMF associations have also been correlated with reduced root parasitism by plants such as *Striga* and *Orobancha*, perhaps due to changes in strigolactones in root exudates that result from AMF colonization (Lopez-Raez, Pozo, & Garcia-Garrido, 2011).

Because the aerial parts of AMF-colonized plants are much easier to study than are root systems hidden belowground, most research has focused on systemically transmitted protection of shoots against insect or pathogen attack. Akin to the discoveries of different pathogen-resistant effects of AMF colonization depending on pathogen lifestyles (Chandanie, Kubota, & Hyakumachi, 2006; De La Noval et al., 2007; Fritz, Jakobsen, Lyngkjær, Thordal-Christensen, & Pons-Kühnemann, 2006; Lee, Lee, & Jeun, 2005; Møller, Kristensen, Yohalem, & Larsen, 2009; Pozo, Jung, López-Ráez, & Azcón-Aguilar, 2010), research into herbivore resistance has also reported differences

that depend on the feeding guild and types of insects involved (Jung, Martinez-Medina, Lopez-Raez, & Pozo, 2012; Pineda et al., 2010). Leaf chewing insects, whose feeding causes extensive tissue damage that triggers jasmonate (JAs)-dependent defensive reprogramming in their hosts, provide an excellent model signalling system for the study of AMF-mediated reinforcement of plant resistance against folivores because many of the mechanisms by which JAs-mediated resistance is mediated are well studied (Howe & Jander, 2008; Schuman & Baldwin, 2016; Wu & Baldwin, 2010). These include both direct and indirect defences, and their priming.

AMF colonization can elicit the release of volatiles from host plants that mediate indirect defences. For example, associations with *Funneliformis mosseae* resulted in enhanced β -ocimene and β -caryophyllene emissions, which increased spider mite predation rates in *Phaseolus vulgaris* (Schausberger, Peneder, Jurschik, & Hoffmann, 2012). AMF colonization can also prime defence responses in host plants, allowing for more rapid and strongly elicited responses (Cameron et al., 2013; Jung et al., 2012; Pineda et al., 2010). AMF-primed defence responses have been reported to confer enhanced resistance against *Fusarium* pathogens in tomato and palm trees (Jaiti, Meddich, & El Hadrami, 2007; Tanwar, Aggarwal, & Panwar, 2013) and the chewing caterpillar, *Helicoverpa arimigera* in tomato (Song et al., 2013). Several recent studies show that AMF networks can transmit damage signals between attacked and unattacked neighbouring plants. In *Vicia faba*, primed but undamaged CMNs-connected neighbouring plants systemically release volatile organic compounds (VOCs) that function as direct defences and repel aphids (Babikova et al., 2013). On the basis of these findings, we infer that plants “eavesdrop” on signals from challenged and AMF-connected neighbours resulting in the priming of defence responses in unchallenged plants. However, alternative explanations can account for the apparent signalling between “donors” and “receivers,” such as interplant signalling mediated directly by volatiles without CMN intervention. To further the analysis of belowground AMF-mediated signalling in plant–herbivore interactions, we used the well-characterized ecological model plant, *Nicotiana attenuata*, whose antiherbivore responses have been particularly well-studied (Schuman & Baldwin, 2016; Wu & Baldwin, 2010) to examine whether JA-mediated defences are propagated through CMNs.

N. attenuata, an annual wild tobacco species native to the Great Basin Desert of the United States, exists in ephemeral populations, which occur most abundantly after fires but also in smaller annually persistent populations found in washes that lack dominant vegetation and their accumulated leaf litter (Bahulikar, Stanculescu, Preston, & Baldwin, 2004). Excavated roots from field-grown plants exhibited the characteristic structures of AMF symbiosis: arbuscules. By sequencing, the AMF species were identified as *Rhizophagus irregularis* and *F. mosseae* (Groten, Nawaz, Nguyen, Santhanam, & Baldwin, 2015; Wang, Wilde, Baldwin, & Groten, 2018). Extensive research with the *N. attenuata* model system has demonstrated that VOCs signals from herbivores-attacked neighbours do not prime neighbouring “receiver” plants, which show no differences in JAs levels or any other defensive traits elicited by treating puncture wounds with oral secretions (OS) from *Manduca sexta* larvae (Paschold, Halitschke, & Baldwin, 2006).

As a consequence, *N. attenuata* is an ideal system for investigating the potential for the priming of herbivore resistance through CMNs.

Here, we use *N. attenuata* to study the potential for herbivory-elicited priming mediated by a belowground mycorrhizal network, without the potentially confounding influence of aboveground VOC-mediated signalling. Given the pivotal roles of JAs in herbivore defence in general, and in particular, in *N. attenuata* (Howe & Jander, 2008; Wu & Baldwin, 2010), we first conducted an initial comparison of multiple host plant species associating with AMF grown in monocultures in the glasshouse. Increases in constitutive JAs levels in AMF-colonized roots were found in two Solanaceous species, including *N. attenuata*, which were associated with accumulations of JA-mediated defence metabolites in the infected roots. However, these increases did not translate into defence increases in systemic leaves, either in basal jasmonate levels, JA-dependent secondary metabolites, or OS-elicited JA bursts when plants were grown in monoculture with AMF. To better understand *N. attenuata*'s defensive responses when connected by CMNs to other plants in a community, a mesocosm system was designed to prevent direct root contact but allow for interplant connections only via the AMF CMNs. This mesocosm system was designed to explore the OS-elicited responses in "receiver" plants that were either connected by CMNs to previously OS-elicited plants or not.

2 | MATERIALS AND METHODS

2.1 | *N. attenuata* seed germination and growth

In all experiments, *N. attenuata* seeds (Torr. ex S. Wats.) of the 31st generation inbred line were used. Seed germination and plant growth were performed as described (Krugel, Lim, Gase, Halitschke, & Baldwin, 2002; Wang, Schäfer, et al., 2018). *N. attenuata* seeds were sterilized and germinated on agar with Gamborg B5 (Duchefa, the Netherlands, <http://www.duchefa.com>) after soaking for 1 hr in a 1:50 (v/v) diluted liquid smoke (House of Herbs, Passaic, NY, USA) supplemented with 1 mM of gibberellic acid (GA₃). Seedlings were grown in Percival chambers at 28°C, under long-day conditions (16 hr light/8 hr dark). Ten days later, seedlings were transfer to TEKU pots for another 10 days of growth, when size-matched young seedlings were planted into pots or mesocosm chambers.

2.2 | Multiple plant species mycorrhizal inoculations

N. attenuata, *Solanum lycopersicum* "Moneymaker," *Hordeum vulgare* "Elbany," *Triticum aestivum* "Chinese Spring," and *Medicago truncatula* leaves and roots (Figure 1) were obtained from the same samples described in Wang, Schäfer, et al. (2018). All plants were grown in a glasshouse with a day:night temperature regime of 28°C (16 hr):26°C (8 hr) and supplemental light from Philips Sun-T Agro 400 W or 600 W Na lights.

For the *R. irregularis* inoculation experiments, the inoculum originated from Biomyx Vital (BioMyc, Germany), which was diluted 1:10

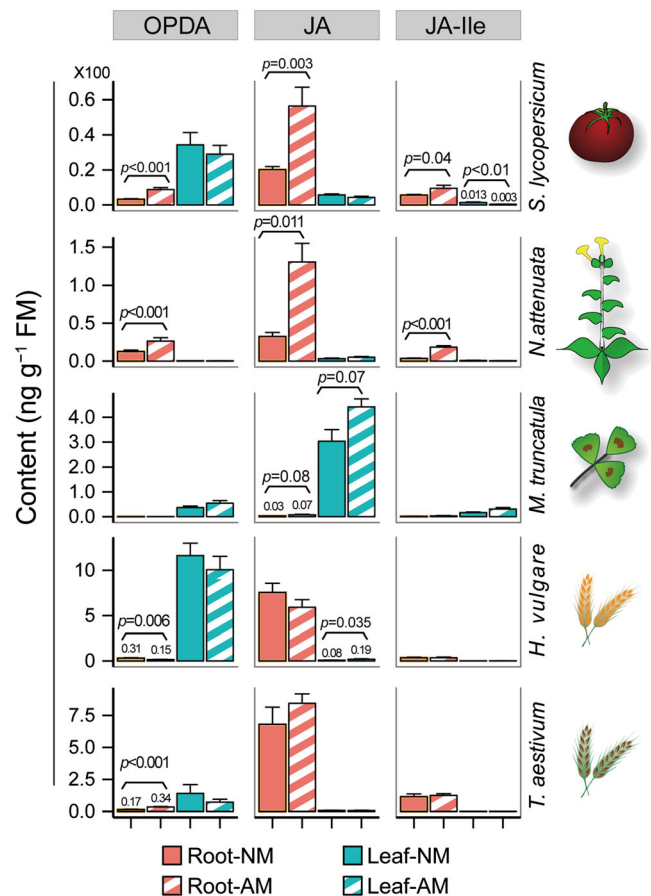


FIGURE 1 AMF inoculation increases constitutive jasmonate levels in the roots of Solanaceous plants. *Nicotiana attenuata*, *Solanum lycopersicum*, *Triticum aestivum*, *Medicago truncatula*, and *Hordeum vulgare* plants were inoculated with (AM) or without (NM) *Rhizophagus irregularis* and cultured under the same growth conditions in a glasshouse. Root and leaves were harvested when plants were in the same stage of growth at the indicated weeks postinoculation (wpi). Data are means (\pm SD) of replicate plants; statistical differences between inoculated and noninoculated plants were evaluated with Student's *t* tests: *N. attenuata* ($n = 8$, 6 wpi); *S. lycopersicum* ($n = 10$, 8 wpi); *M. truncatula* ($n = 4$, 7 wpi); *H. vulgare* ($n = 6$, 8 wpi), and *T. aestivum* ($n = 10$, 8 wpi)

with autoclaved expanded clay (Lecaton, 2- to 5-mm particle size), or autoclaved inoculum (at 121°C for 30 min) mixed with expanded clay in a 1/10 ratio as a control group. Plants were watered with a hydroponic fertilizer solution with 1/10 of the regular inorganic P_i content, while plants were in the rosette stage of growth, which was replaced with 1/4 P_i concentration when the plants entered the elongation stage. Leaf and stalk lengths were recorded every 3 days (Figure 3b).

2.3 | Experimental mesocosm design and mycorrhizal inoculation

To create replicate *N. attenuata* communities in which AMF interactions among members could be experimentally controlled, a mesocosm

consisting of four single-plant boxes was designed. Each mesocosm consisted of four plastic boxes (length:width:height = 9.5:9.5:24 cm) separated by metal mesh (pore diameter = 30 μm), which excluded root contact among plants but allowed passage of AMF mycelia (Figure S2). In each mesocosm, the 4.5-cm spaces that separated the four boxes from each other were occupied by *N. attenuata* WT “nurse plants” inoculated with either autoclaved or live *R. irregularis* inoculum. Previous experiments had established that 4 weeks of growth of these nurse plants activated and generated a very strong source of inoculum that rapidly established a CMN among the four experimental plants of each mesocosm. The nurse plants were grown for 4 weeks, and just prior to the planting of the experimental plants into the individual boxes, the nurse plants were removed (Figures 3a and S2). The fungus concentration was evaluated by measuring AMF-indicative blumenol metabolites (Wang, Schäfer, et al., 2018) in the leaves of the nurse and experimental plants. Once the nurse plants were removed, the experimental plants were transferred into their individual boxes, for an additional 5 weeks of growth before the start of experimentation. The four individual plants of each mesocosm were named “donor” and “receiver” plants 1 to 3 (Figures 3a and S2).

2.4 | Experimental mesocosm groups

Mesocosms were assigned to four experimental groups (Con1, Con2, Con3, and T) based on whether live AMF inoculum was absent or present in the nurse plant space and whether experimental “donor” plants were elicited by immediately treating puncture wounds (W) produced by a fabric pattern wheel with 1/4 diluted aqueous OS (20 μl) from *M. sexta* larvae (Figures 3a and S2). The OS-elicitation procedure allows for the activation of both systemic and local antiherbivore responses in a highly standardized and synchronized manner (Halitschke, Gase, Hui, Schmidt, & Baldwin, 2003). Each mesocosm was a biological replicate. The four treatment groups were as follows:

Con1: autoclaved AMF inoculum was used (N), “donor” plants were treated with W + OS (Y);

Con2: active AMF inoculum was used, but 1 week prior to W + OS treatment of the “donor” plants, the interconnecting AMF mycelial network was removed by emptying the nurse plant space of soil (Y/R), the “donor” plants were treated with W + OS (Y);

Con3: active AMF inoculum was used (Y), but “donor” plants were not treated with W + OS (N);

T: active AMF inoculum was used (Y), “donor” plants were treated with W + OS (Y).

In Con1, “donors” were elicited with W + OS but lacked CMNs connecting neighbours, whereas the opposite was the case for the plants of mesocosm Con3. AMF associations can result in significant differences in plant growth, and substantial differences in plant size can occur among plants grown with and without AMF networks (AM/NM), and these differences in size can confound defence

response differences as defence metabolites accumulate according to metabolite-specific allometric relationships (Baldwin & Karb, 1995). As AMF associations can change plant size compared with uncolonized plants, it was important to create unconnected networks of plants of the same size relative to group T plants in order to compare defence responses. To this end, mesocosm Con2 was created;

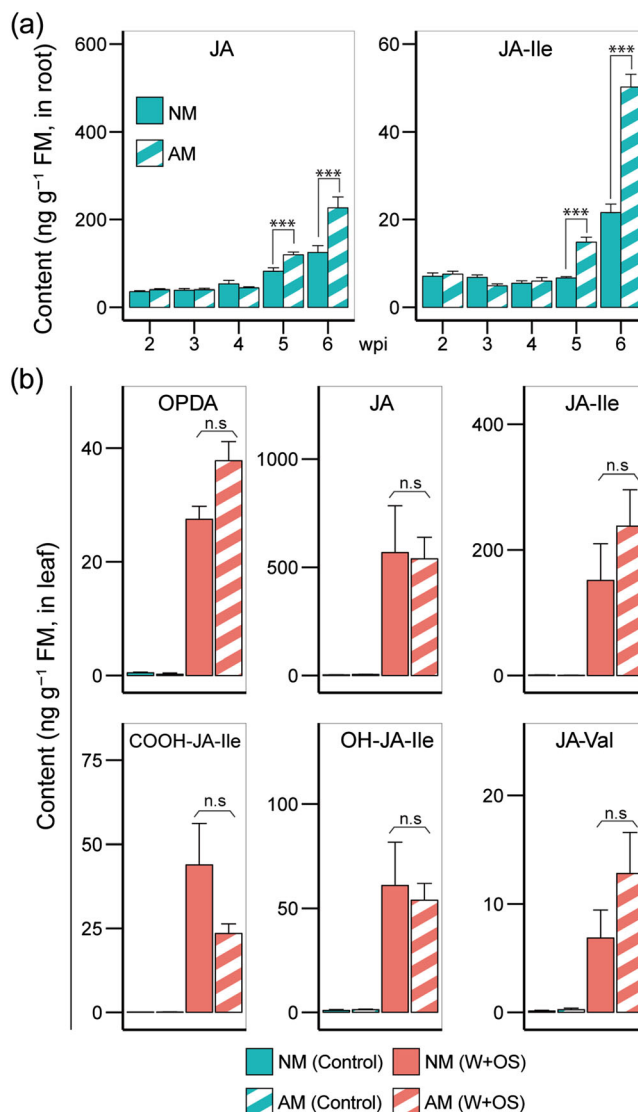


FIGURE 2 Increased JA and JA-Ile levels in the roots of *Nicotiana attenuata* associated with AMF inoculations do not influence the magnitudes of the JA bursts in leaves elicited by the treatment of leaf puncture wounds (W) with oral secretion (OS) from *Manduca sexta* larvae. (a) Root samples were harvested from a time-series experiment of plants harvested at weekly intervals, 2–6 weeks postinoculation (wpi). Data are means (+SD, $n = 6$) of plants grown individually in pots with or without AMF inoculum. Student's t test ($*p \leq .05$, $**p \leq .01$, $***p \leq .001$). NM, absence of AMF (solid); AM, presence of *Rhizophagus irregularis* inoculum (hatched). (b) Detailed jasmonate metabolism profiling revealed a dramatic JA burst after W + OS treatment, which did not differ significantly between AMF inoculated (AM, hatched bars) and control noninoculated plants (NM, solid bars); data are means (+SD, $n = 5, 6$ wpi) of individual plants

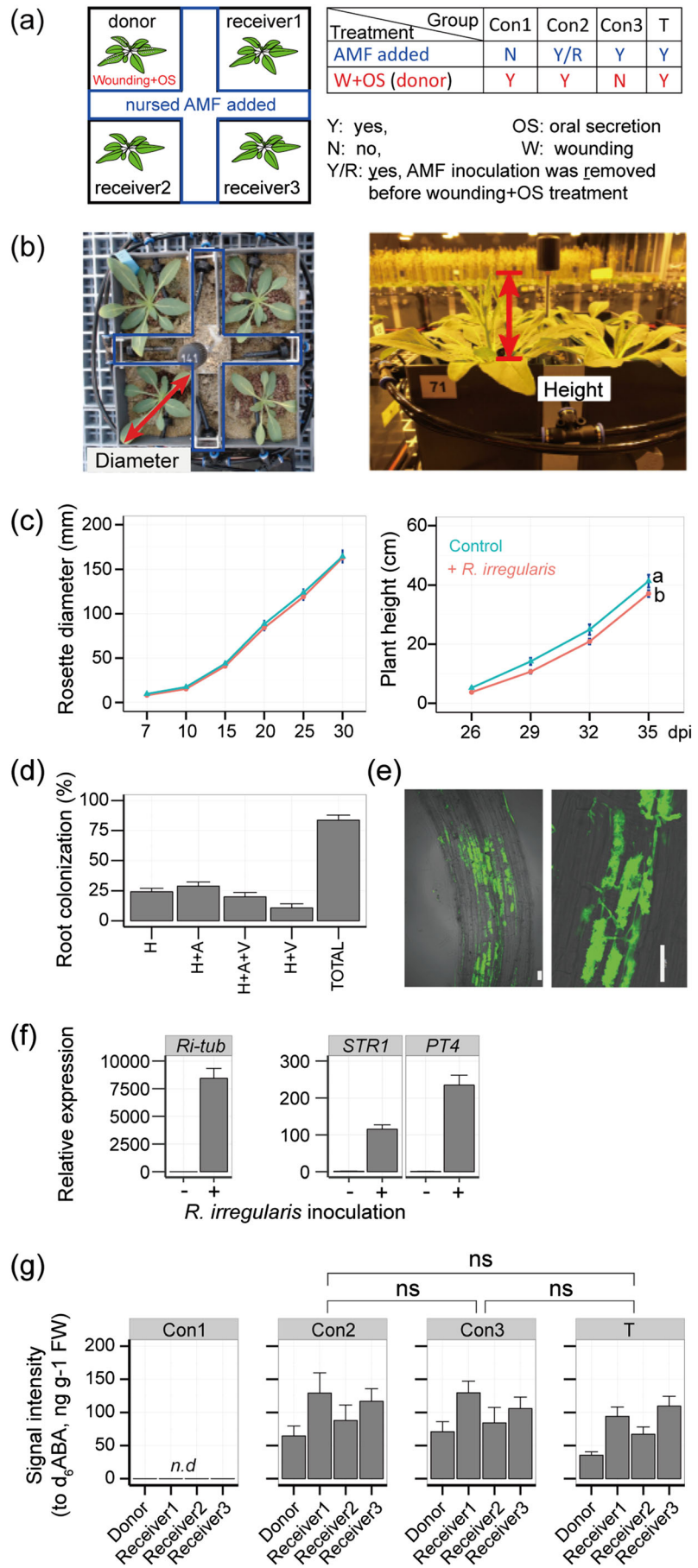


FIGURE 3 Design of experimental mesocosms and mesocosm treatment groups to which replicate mesocosms was assigned and growth and AMF root colonization of plants in the mesocosms and treatments. (a) Four individual plants (“donor” and “receivers” 1 to 3) comprised each replicate mesocosm. Each mesocosm was assigned to one of four different combinations of AMF addition and W + OS elicitations (Con1-4, T) described in Table (right). See Figure 4a for the timing of the elicitations and harvests of the mesocosm plants. (b) Representative pictures of plants growing in the mesocosms. Rosette diameters (left red arrows) were measured throughout the rosette stage of growth; plant heights (right red arrows) were measured throughout the elongation stage of growth. (c) Mesocosms plants were classified into two groups: AMF-free (NM, blue line) and AMF-inoculated (AM, red line). Differences in diameters of rosette-stage plants were not significantly different between these two groups, but stalk elongations of AMF-inoculated plants were slower than those of AMF-free plants. Different letters indicate significant differences ($p < .05$, one-way ANOVA followed by Tukey’s HSD: NM plants, $n = 24$; AM plants, $n = 84$). (d) Four randomly selected replicates were examined for microscopic characterizations of AMF root colonization of AMF-harboring groups (Con2, Con3, and T): H, hyphae; A, arbuscules; V, vesicles; T, total colonization. (e) Representative pictures from WGA fluorescence staining, raw images were captured by LSM META510, scale bars = 50 μM . (f) Transcript abundance analysis of AMF-indicative marker genes, including *Ri-tubline*, *NaSTR1*, *NaPT4* (relative to *IF5a*). Data are means (+SD; “-” $n = 4$; “+” $n = 12$). (g) Leaf hydroxyblumenol C-glucoside contents, a leaf marker of AMF associations in the roots (Wang, Schäfer, et al., 2018) were quantified from leaves of all plants in all treatments. Data are means (+SD: Con1, $n = 6$; Con2, $n = 7$; Con3, $n = 7$; T, $n = 7$), statistical differences among AMF-inoculated groups are analysed by one-way ANOVAs followed by Tukey’s HSD ($p \leq .05$). n.d., not detected; ns, not significant

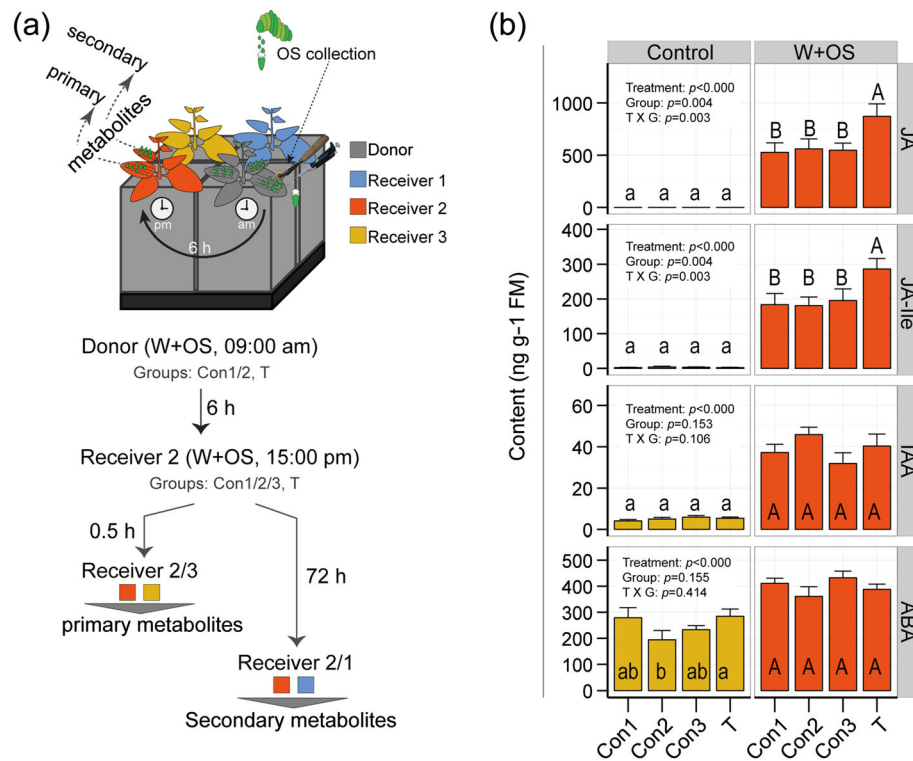


FIGURE 4 Evidence of AMF-mediated defence priming mediated by AMF networks: JA and JA-Ile bursts were amplified in the “receiver” plants of the AMF mycelia group (T) after the W + OS elicitation of the “donor” plants. (a) Schematic illustration of the experimental set-up, treatment sequence and data analysis. Each replicate mesocosm consisted of one “donor” plant and three “receiver” plants. Three leaves of each “donor” plant (grey) from mesocosm groups Con1, 2 and T were elicited with W + OS at 9:00 am. Six hours later, when the hypothetical AMF-mediated signal had been transmitted from “donor” to “receiver” plants, two leaves of each “receiver” 2 plants (orange) in all four mesocosm groups were also W + OS elicited; 0.5 hr later, one of the treated leaves from “receiver” 2 (orange) and one leaf from untreated “receiver” 3 plant (yellow) as a control were harvested for phytohormone and primary metabolite measurements; the other treated leaf from “receiver” 2 plants (orange) and one leaf from untreated “receiver” 1 plants (blue) as controls were harvested at 72 hr for secondary metabolites profiling. (b) Phytohormones JA, JA-Ile, IAA, and ABA were quantified. Data are means (+SD, for each mesocosm group replicate: Con1, $n = 6$; Con2, $n = 7$; Con3, $n = 7$; T, $n = 7$). Different letters indicate significant differences ($p < .05$, one-way ANOVA followed by Fisher’s LSD). n.d., not detected

all plants in groups Con2 and T were grown similarly, but the hyphal network was disconnected just prior to OS elicitation by removing (with a vacuum cleaner) the soil and hyphae from the “nurse plant” space in Con2 (Figure 3a). Before mesocosms were allocated to AMF-treatment groups (Con2, Con3, and T), the intensity of root colonization was evaluated by measuring content of AMF-indicative blumenol compounds, and only the mesocosms that showed similar root colonization were used (see Figure 3g).

2.5 | Mesocosm experimental W + OS treatment procedure

Five weeks after transferring the experimental plants into mesocosms, all four groups were treated and harvested in the same way (Figure 4 a): 6 hr after “donor” plants were W + OS elicited, OS-elicited “receiver 2” and untreated “receiver 3” leaves were harvested to quantitatively test the hypothesis that the mycorrhizal network transmits damage signals that prime the JAs burst (and amino acid levels) in CMN-connected donors. This experimental design therefore extends the hypothesis tested in the previous experiments, which found OS-

elicited JA bursts not to be primed by simple mycorrhization alone (Figure 2). After quantification of the JAs burst 30 min after OS elicitation, the slower responding secondary metabolites were quantified in OS-elicited “receiver 2” and untreated “receiver 1” leaves 72 hr after the OS elicitation (Figure 4a); these analyses required a separate “receiver 1” as a control to ensure that the leaf sampling itself did not confound any potential AMF-mediated priming.

The timing of the treatments was as follows (see Figure 4a): in the morning (09:00) on the day of treatment, “donor” plants in the Con1, Con2, and T treatment mesocosms were W + OS elicited on three stem leaves (fourth, fifth, sixth, basal to apical) to generate sufficient signals for systemic signalling in undamaged but AMF-connected plants. Six hours later (15:00 p.m.), two leaves were W + OS elicited of each “receiver 2” plant in all four groups. The two treated stem leaves were specifically selected from the same positions (fourth, sixth, basal to apical). All treated fourth leaves from each “receiver 2” and “receiver 3” plants, as controls, were harvested 0.5 hr later (15:30 p.m.) for the quantification of primary metabolites measurements. After 72 hr (15:00 p.m., +3 days), the treated sixth leaf from each “receiver 2” plant along with a leaf in an identical position of

"receiver 1" plants was harvested for secondary metabolite quantifications (see Figure 4a for a summary of the sampling schedule).

2.6 | Samples harvest, root staining, and colonization assessment

Freshly harvested roots were chopped into approximately 1-cm-long pieces and stored in a storage solution consisting of 99% ethanol and 60% aqueous acetic acid (3:1, v:v) at 4°C; stem leaves from the same positions as well as the rest of the root material were flash-frozen in liquid nitrogen.

For fungal colonization estimation, roots were rinsed twice with distilled water from the storage solution, cleared with 20% KOH (96°C, 5 min), rinsed and finally acidified with 2% HCL for 5 min at 96°C before being stained with a 0.05% trypan blue solution (lactic acid:glycerol:distilled water [1:1:1, v:v]). After an overnight destaining step, roots were stored in glycerol:lactic acid:distilled water (1:1:1, v:v) until mounted on slides for microscopic examinations. Root AMF colonization was evaluated using the method described by Brundrett, Piche, and Peterson (1984). Briefly, more than 150 viewfields per slide were surveyed with a 20× objective magnification of a regular optical microscope and classified into five groups: no colonization, only hyphae (H), hyphae with arbuscules (H + A), hyphae with vesicles (H + V), and hyphae with arbuscules and vesicles (H + A + V). The proportions of each group were normalized by the total views. Fluorescence staining was used to visualize the inoculation structures, and trypan blue was substituted by wheat germ agglutinin-Alexafluor 488 (0.2 mg/ml) for overnight incubation at room temperature in dark (Vierheilig, Schweiger, & Brundrett, 2005). After a quick washing with distilled water, root samples were mounted on slides and a Zeiss confocal microscope (LSM 510 META, Zeiss, Jena, Germany) was employed to detect (excitation/emission maxima at approximately 495/519 nm) AMF-associated structures.

2.7 | Total RNA extraction and transcript abundances analysis

For the molecular biological analysis of colonization rates, RNA was extracted from the roots (~100 mg) using the RNAeasy Plant Mini Kit (Qiagen) or NucleoSpin® RNA Plant (Macherey-Nagel) according to the manufacturer's instructions and cDNA was synthesized by reverse transcription using the PrimeScript RT-qPCR Kit (TaKaRa). Quantitative (q)PCR was performed on a Stratagene Mx3005P qPCR machine using a SYBR Green containing reaction mix (Eurogentec, qPCR Core kit for SYBR Green I No ROX). Primer sequences are listed in Table S2.

2.8 | Primary and secondary metabolites extraction and analysis

For primary and secondary metabolites extraction, leaf samples were aliquoted into reaction tubes and their masses were recorded for normalization. Per 100-mg plant tissues, 1-ml extraction buffer (80%

MeOH with internal standards) was pipetted into the samples before being shaken in a GenoGrinder 2000 (SPEX SamplePrep) for 60 s at 1,150 strokes. After two centrifugations, the supernatant was collected and analysed following the procedures described by Schäfer, Brütting, Baldwin, and Kallenbach (2016).

For primary metabolites analysis, including the phytohormones, jasmonic acid (JA), JA-Ile, abscisic acid (ABA), and indole-3-acetic acid (IAA), amino acids in Figure 5, and secondary metabolites in Figure S1, a detailed method described by Schäfer et al. (2016) was used. In brief, for chromatographic separations, an ultrahigh performance liquid chromatograph (UHPLC; Dionex UltiMate 3000) equipped with a reverse phase column (Agilent ZORBAX Eclipse XDB C18, 50 × 3.0 mm, 1.8 μm) as the stationary phase was used. Mobile phases containing A, 0.05% HCOOH, 0.1% ACN in H₂O and B, MeOH, were optimized for separation and analysis speed. Analysis was performed on a Bruker Elite EvoQ triple-quadrupole MS equipped with a HESI (heated electrospray ionization) ion source. Contents of the metabolites were quantified by use of internal standards of their own stable isotope-labelled products including D₆-JA, D₆-JA-Ile, D₆-ABA, D-IAA, and different labelled-amino acids products as internal standards (Schäfer et al., 2016). For the quantification of compounds without isotope-labelled internal standards, COOH-JA-Ile, OH-JA-Ile, and JA-Val concentrations were calculated relative to D₆-JA-Ile and OPDA concentrations relative to D₆-JA, and for the secondary metabolites depicted in Figure S1, the concentrations of caffeoylputrescine (CP), chlorogenic acid (CGA), and the associated metabolites involved in the biosynthetic pathways of CP and CGA, namely, shikimic acid, caffeic acid, cinnamic acid, ferulic acid, sinapic acid, and rutin, were calculated relative to the D-IAA internal standard.

For hydroxyblumenol C-glucoside measurements in Figure 3g, the detailed method described by (Mindt, Wang, Schäfer, Halitschke, & Baldwin, 2019) was used. In brief, 80% MeOH extracts spiked with stable isotope-labelled abscisic acid (D₆-ABA, HPLC Standards GmbH) as an internal standard were measured with a Bruker Elite EvoQ triple-quadrupole MS.

For the quantification of 17-hydroxygeranylinalool diterpene glycosides (HGL-DTGs) depicted in Figure 7 and other secondary metabolites in Figure 6, UHPLC (Dionex UltiMate 3000 rapid separation LC system; Thermo Fisher) with a Thermo Fisher Acclaim RSLC 120 C18, 150 × 2.1 mm, 2.2 μm column, was used. The mobile phases changed from a high % A (water with 0.1% acetonitrile and 0.05% formic acid) in a linear gradient to a high % B (acetonitrile with 0.05% formic acid) followed by column equilibration steps and a return to starting conditions. The flow rate was 0.3 ml/min. MS detection was performed using a microTOF-Q II MS system (Bruker Daltonics), equipped with an electrospray ionization (ESI) source operating in positive ion mode. ESI conditions for the microTOF-Q II system were end plate offset 500 V, capillary voltage 4500 V, capillary exit 130 V, dry temperature 180°C, and a dry gas flow of 10 L min⁻¹. Mass calibration was performed using sodium formiate (250-ml isopropanol, 1-ml formic acid, 5-ml 1M NaOH in 500-ml water). Data files were calibrated using the Bruker high-precision calibration algorithm. Instrument control, data acquisition, and reprocessing were performed using HyStar 3.1 (Bruker Daltonics).

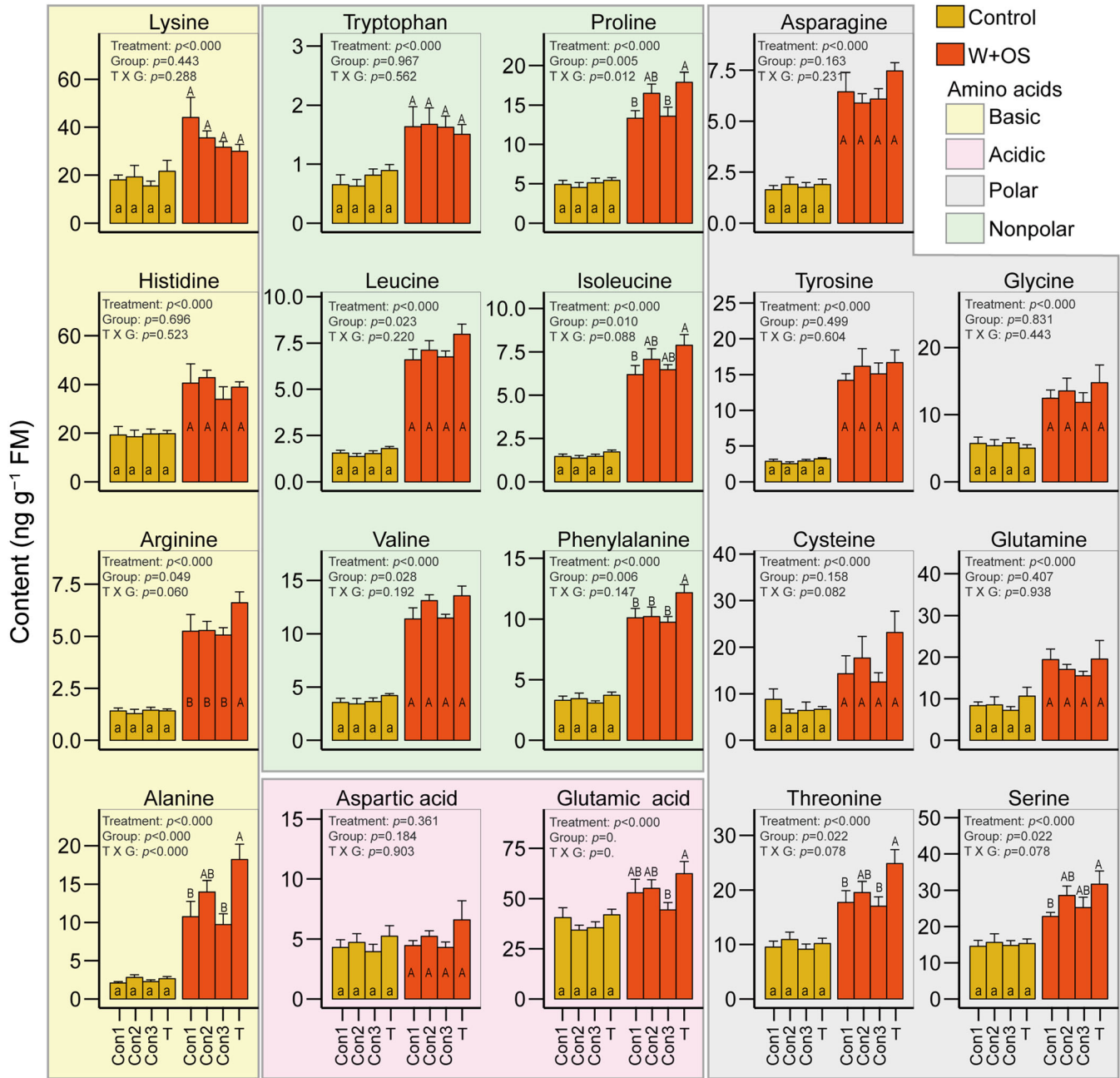


FIGURE 5 W + OS elicitation results in changes in amino acid levels that differ among the four mesocosm groups. Overall, treated samples (W + OS, orange bars) were highly elevated in amino acid accumulations compared with the unelicited controls (yellow bars). Some of the defence-associated amino acids, such as threonine, arginine and phenylalanine, were more strongly elevated in mesocosm group T. The biological replicates employed for amino acid quantification were the same as described in Figure 4. Data are means (+SD; Con1, $n = 6$; Con2, $n = 7$; Con3, $n = 7$; T, $n = 7$). Different letters indicate significant differences ($p < .05$, one-way ANOVA followed by Fisher's LSD). n.d., not detected. Different background colours indicate the types of amino acids: basic, acidic, polar, and nonpolar

2.9 | Statistical analysis

One-way ANOVAs were performed among groups (Con1, Con2, Con3, and T), followed by either Tukey's HSD or Fisher's LSD. Two-way ANOVAs were performed between treatments (control/W + OS) and groups. Student's *t* test was applied for comparisons of two groups.

3 | RESULTS

3.1 | JAs levels in AMF-colonized roots increase in two Solanaceous species

Three jasmonates, including jasmonic acid (JA), 12-oxo-phytodienoic acid (OPDA), and JA-Ile, were examined in both leaves and roots of

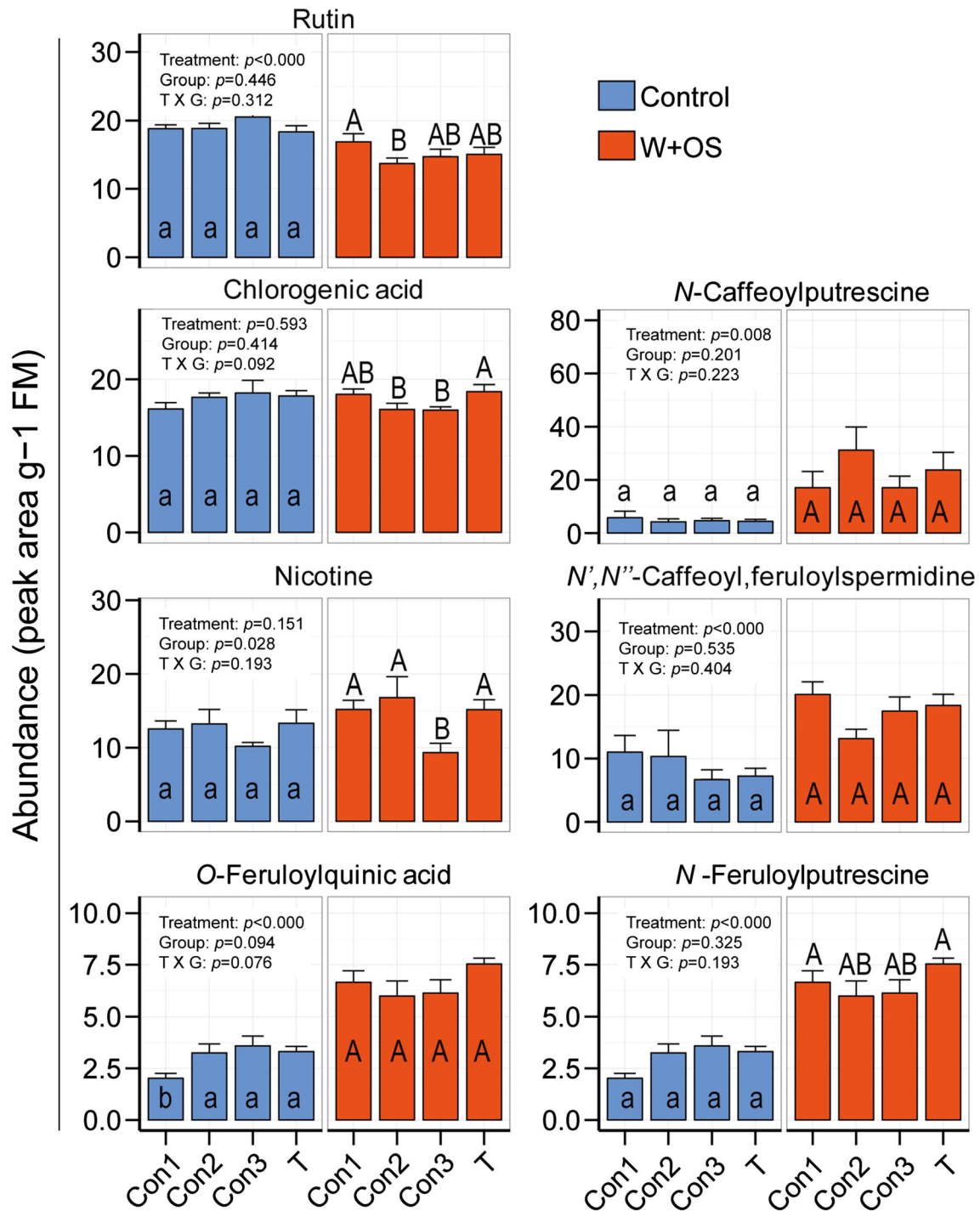


FIGURE 6 The W + OS inducibility of different antiherbivory defence compounds do not differ among the four treatment groups. Accumulation of defence compounds such as nicotine, chlorogenic acid and rutin did not differ among the four mesocosm groups. Well-characterized phenolamides such as caffeoylputrescine were induced to higher levels after W + OS elicitation (orange) relative to unelicited controls (blue). Data are means (\pm SD; Con1, $n = 6$; Con2, $n = 7$; Con3, $n = 7$; T, $n = 7$). Different letters indicate significant differences ($p < .05$, one-way ANOVA followed by Fisher's LSD)

five plant species with or without AMF inoculation (Figure 1). In general, the abundance of the three jasmonates varied with tissues and species. For example, in *Medicago* roots, the contents of JA, OPDA, and JA-Ile were much lower than those in the leaves. In the monocots,

only OPDA increased in wheat roots after AMF inoculation, but in barley, OPDA concentrations decreased in roots, whereas JA levels increased in leaves (Figure 1). No significant changes in jasmonate levels were detected in *Medicago* (Figure 1). In both of the solanaceous

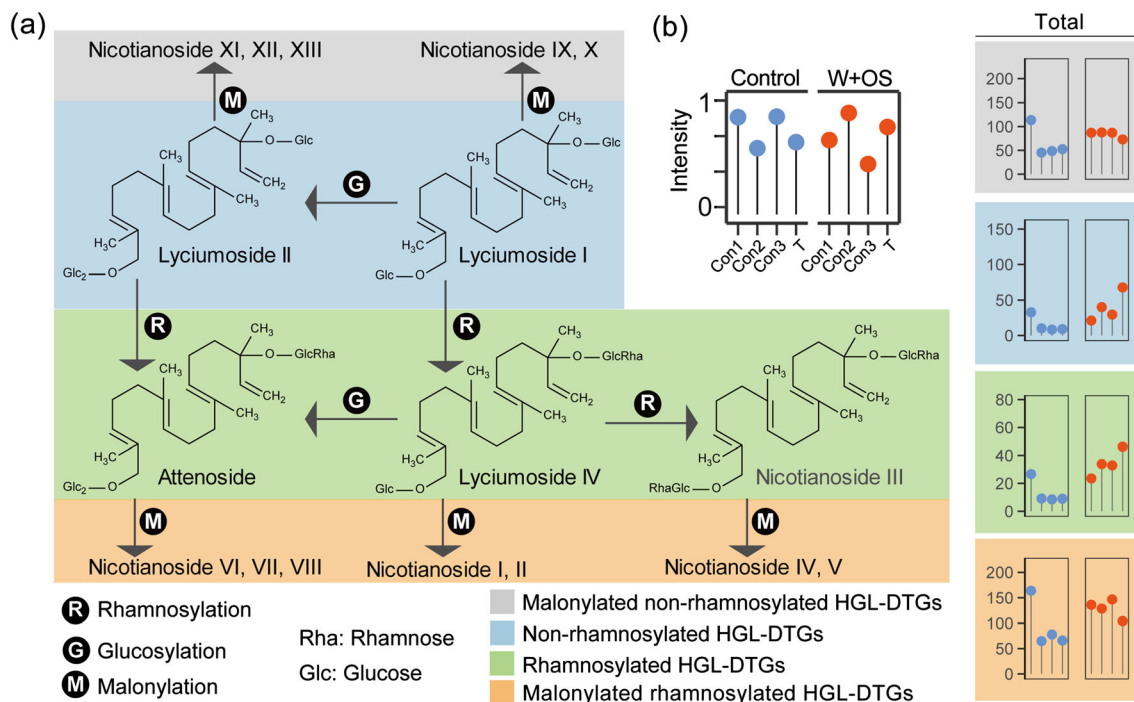


FIGURE 7 Hydroxygeranylinalool diterpene glycosides (HGL-DTGs) exhibit compound-specific increases in response to W + OS elicitation among the four mesocosm groups. In general, leaf concentrations of HGL-DTGs were significantly lower in AMF-inoculated plants of “receiver” 1, but after OS elicitation, compound-specific differential induction was clearly discernible among the four mesocosm groups. (a) Schematic illustration of the simplified HGL-DTGs biosynthetic pathway, different biosynthetic steps are indicated by black arrows. Legend for lollipop charts (right corner) indicates the different treatments (x axis) and relative concentrations of compounds (y axis). The data from the same compound class are grouped together with same background colour. (b) Compounds from the same compound class were summed to provide a total amount, and all of the quantified HGL-DTGs were summed to provide an overall-total HGL-DTG value. For the concentrations of individual compounds see Figure S3. All of the biological replicates used for the DTG analysis are the same as described in Figure 6. Data are means (+SE; Con1, $n = 6$; Con2, $n = 7$; Con3, $n = 7$; T, $n = 7$). For results of the statistical analysis see Table S1

species, a consistent increase of all three compounds in roots was found after AMF inoculation, but much lower levels were found in leaves, which did not differ significantly between AMF-inoculated and uninoculated plants (Figure 1).

To further evaluate the increase in jasmonates in AMF colonized roots of *N. attenuata*, a time-series experiment was conducted with WT plants. Jasmonate levels (JA and JA-Ile) in the roots of all plants prior to the flowering stage of growth (2/3/4 weeks postinoculation [wpi]) did not differ, regardless of AMF colonization, but at 5 wpi when plants had started flowering, root JA and JA-Ile levels increased in AMF-colonized roots (Figure 2a). Two-way ANOVAs were performed between treatments (control/W + OS) and groups. Student's *t* test was applied for comparisons of two groups (Figure 2a). This time-series experiment revealed that the jasmonate responses in *N. attenuata* roots depend very much on the plants acquiring a fully mature AMF network, which under the glasshouse conditions used here, occurs at 5 wpi.

We also compared the JA-regulated metabolic changes (Figure S1a) in *N. attenuata* that resulted from AMF associations in root and leaf tissues separately. In general, the abundances of most metabolites exhibited tissue-dependent patterns; for example, rutin was highly enriched in leaves, and far lesser amounts were detected in roots (around 1/1000; Figure S1b). In contrast, constitutive JA and JA-Ile contents were readily detected in the roots, but far lower amounts

were found in unelicited leaves, and these values were so low that they were at the limit of detection and hence thwarted accurate quantification (Figure S1b). In root tissues, rutin, phenylalanine, and caffeoylputrescine (CP) levels were not significantly altered in response to *R. irregularis* inoculation (Figure S1b). For all of the remaining root metabolites, such as caffeic acid, consistent significant increases were found with differential fold-increases (Figure S1b).

In contrast to the responses in the roots, AMF inoculation largely did not change the concentrations of most leaf metabolites, with a few exceptions: *R. irregularis* inoculation increased arginine levels but decreased levels of ferulic acid and rutin (Figure S1b). Overall, AMF-colonized roots harboured higher concentrations of a majority of the quantified metabolites, but only sporadic changes were observed in systemic leaves. These results suggested that the large increases in the concentrations of jasmonates in mycorrhizal roots did not translate into systemic increases in JA-regulated phenolic defences in leaves.

3.2 | Constitutive AMF-mediated increases in root jasmonates do not amplify OS-elicited JA bursts in leaves

Our previous research demonstrated that when tomato plants associated with *F. mosseae* (syn. *Glomus mosseae*), transcripts of defence-

related genes were increased (Song et al., 2013). To evaluate if similar responses occurred in the *N. attenuata* system, we used the most reliable marker of herbivore-elicited defence response in this system: the OS-elicited JA burst. We first compared OS-elicited JA bursts in plants grown with (AM) and without (NM) AMF inoculum (*R. irregularis*). In NM plants, W + OS elicitation rapidly induced JA bursts in 0.5 hr, increasing JA (~500 times) and JA-Ile (~200 times) levels in treated leaves with similarly rapid increases in JA-related intermediates including OPDA, COOH-JA-Ile, OH-JA-Ile, and JA-valine (Figure 2b). However, these OS-elicited JA bursts in AM plants did not differ significantly from those quantified in NM plants (Figure 2b). From these results, we conclude that in *N. attenuata* plants, the OS-elicited jasmonates burst in leaves is not amplified by mycorrhization, even if constitutive jasmonates level is increased in AMF-colonized roots.

3.3 | CMNs are established among plants in the laboratory mesocosm

To examine defence signal transfer among CMN-connected *N. attenuata* plants, a laboratory mesocosm was constructed and tested (Figures 3a and S2). The growth of AMF-inoculated plants was slower than that of AMF-free plants though no obvious differences were detected in plant diameter, consistent with an inhibitory effect of mycorrhizal association (Figure 3b,c) as described previously for this system (Riedel, Groten, & Baldwin, 2008). All examined AMF-inoculated plants were well colonized ($n = 12$): total root colonization was about 80%, and the core structure, arbuscules were about 45% (Figure 3d). Arbuscules were clearly observed after florescence staining in AMF-inoculated plants (Figure 3e). Transcript abundance of AMF-indicative molecular markers including *Ri-tubulin*, *NaPT4*, and *NaSTR1* were dramatically increased by AMF inoculation (Figure 3f), suggesting that a robust mycelial network linking plants had been established among the plants in the mesocosms. We further examined this inference across all 108 individual plants by quantifying the levels of hydroxyblumenol-C-glucosides in leaves, a root colonization-indicative chemical marker (Wang, Schäfer, et al., 2018). No detectable amounts occurred in NM plants, but in all AM plants, hydroxyblumenol-C-glucosides increased with AMF associations, which indicated overall comparable connectedness between “donor” and “receiver” plants among mesocosm groups, though the concentrations varied among mesocosms or among the four plants within a single mesocosm (Figure 3g).

3.4 | W + OS-elicited JA bursts are primed in the leaves of neighbouring plants with CMNs connections to previously W + OS-elicited plants

In order to evaluate if the CMN transmits OS-elicited signals among plants, the rapid JA and amino acids changes and slower changes in secondary metabolites were quantitatively analysed in “receiver” plants: 0.5-hr OS-elicited “receiver 2” plants were compared with “receiver 3” control plants; 72-hr OS-elicited “receiver 2” plants were

compared with “receiver 1” control plants, as explained above (Figure 4a). As expected, constitutive jasmonate levels in “receiver 3” plants were similar among four mesocosm groups. The 0.5-hr OS-elicited JA bursts of the three “receiver 2” plants of mesocosm groups Con1, Con2, and Con3 did not differ statistically (Figure 4b), whereas those of group T were approximately 1.5-fold larger in all components of the active parts of the JA burst, including JA and JA-Ile (Figure 4b). Note that W + OS-elicited JA burst of plants directly associated with AMF and grown in monocultures did not exhibit this amplification (Figure 2b). In contrast to the active parts of the JA burst, the deactivation steps in JA signalling, namely, OH-JA-Ile, COOH-JA-Ile, and JA-Val did not differ significantly among the four mesocosm groups (Figure S3).

The importance of IAA and ABA in the herbivore resistance of *N. attenuata* has been recently recognized (Dinh, Baldwin, & Galis, 2013; Hettenhausen, Baldwin, & Wu, 2013; Machado et al., 2016), and these two phytohormones were also quantified after W + OS elicitation. In all W + OS-elicited leaves, IAA and ABA levels were significantly increased, 8- and 1.5-fold respectively (Figure 4b), compared with the levels found in unelicited leaves, but there were no significant differences in the increases of these phytohormones among the four groups (Figure 4b). Amino acids (AA) were also measured and the most basic- or polar AA, but not the acidic AAs (such as aspartic and glutamic acid) increased about 1.5- to 5-fold after OS elicitation (Figure 5). Of the OS-responsive AAs, arginine (Arg) and threonine (Thr) showed a 1.1- and 1.3-fold respective increase in the “receiver 2” plants of mesocosm group T relative to other three mesocosm groups. Nearly all of the hydrophobic amino acids, with the exception of tryptophan, exhibited larger increases in group T “receiver 2” plants after OS elicitation (Figure 5). The group T-responding AAs, including Thr, Arg, and phenylalanine (Phe), are known to be closely associated with jasmonate and phenolamides metabolism.

Taken together, these results revealed that the magnitudes of the JA and associated AA bursts were significantly larger in mesocosm group T “receiver 2” plants. From these significant increases, we infer that these plants had been “primed” in a primary metabolic layer of their defence responses via their connections to the CMNs by the OS elicitation of their connected “donor” plants. To test this inference further, we quantified the levels of defence metabolites, which are known to be activated by JA bursts in these “receiver 2” plants.

3.5 | Phenolamides and HGL-DTGs are examples of primed inducible defences in CMNs-connected plants

Verified defensive metabolites in *N. attenuata* were analysed to evaluate if the priming of the W + OS-elicited JA burst was translated into amplified defence responses. Rutin, nicotine, and chlorogenic acid (CGA) were selected as noninducible compounds (Lee, Joo, Kim, & Baldwin, 2017; Li et al., 2017), and as expected, they were nearly at the same levels after OS treatment within the four groups (Figure 6). Although W + OS-elicited larger Arg levels in the “receiver 2” plants of the group T mesocosm plants (Figure 5), one of its down-stream

products, CGA did not differ significantly among the elicited plants of the four mesocosms (Figure 6).

The significantly elevated phenylalanine levels in the “receiver 2” plants of mesocosm group T (Figure 5) turned our attention to its down-stream defenses, the phenolamides (PAs) which are known to be W + OS-elicited defenses in *N. attenuata* (Onkokesung et al., 2012). Amongst the PAs, larger, but nonsignificant changes in CP, O-feruloylquinic acid, *N,N'*-caffeoyl, feruloylspermidine and *N'*-feruloylputrescine levels were detected in mesocosm group T plants, and no significant amplification in mesocosm group T plants was found compared to the plants of the other three mesocosm groups (Figure 6).

17-Hydroxygeranylinalool diterpene glycosides (HGL-DTGs) are a class of diterpene glycosides (DTGs) found in several species of *Nicotiana* that are known to function defensively against lepidopteran larval herbivores (Heiling et al., 2010). Overall, in control leaves harvested from “receiver 1” plants, every HGL-DTG was significantly reduced in plants associating with AMF (mesocosm groups Con2/Con3/T) compared to those of the noninoculated group (Con1) plants (Figure 7, Table S1). In W + OS elicited leaves, the accumulation of total HGL-DTGs did not differ significantly but the patterns of individual HGL-DTGs accumulations were highly different depending on the attached sugar moieties or malonylation modifications of the structures (Figure 7b, Figure S4, Table S1). For example, members containing both nonrhamnosylated (lyciumoside I/II) and rhamnosylated [lyciumoside IV, attenoside and nicotianoside III, but all lacking malonylations, were more strongly W + OS-elicited in the plants of the Con2 mesocosm group (Figure 7b, Figure S4, Table S1). In contrast, two of three side-branches of malonylated rhamnosylated HGL-DTGs including: 1) nicotianoside IV, and V derived from nicotianoside III; 2) nicotianoside VI, VII, and VIII derived from attenoside, were less strongly OS-elicited in mesocosm group T relative to other groups, even though the DTGs from the lyciumoside IV branch, 3) nicotianoside I, II barely changed in abundance in all four groups (Figure 7b, Figure S4, Table S1). The malonylated nonrhamnosylated HGL-DTG also did not change after OS elicitation. Based on these results, we infer that AMF-mediated priming occurs in a highly compound-specific manner for the HGL-DTGs, and that the plants in group T preferentially increased the concentrations of most nonmalonylated compound classes, rather than the malonylated ones.

4 | DISCUSSION

Plants adapt their physiologies to their local environments by responding to environmental information at both individual and community scales (Bazzaz, 1996). Here, we compared herbivore-induced defences in *N. attenuata* in AMF-associating plants growing individually or in CMNs-connected communities. When grown individually, constitutive jasmonates and JA-regulated secondary metabolism were enhanced in the roots by AMF colonization. However, these local increases did not directly translate into stronger defence responses in the leaves when the plants were challenged by W + OS. However,

when grown in mesocosms designed to examine mycorrhizal network-mediated signalling, W + OS elicitation of mesocosm group T “receiver” plants, which were connected by an AMF network to previously W + OS-elicited “donors,” led to larger JA bursts, higher levels of JA metabolism-associated amino acids, and in particular, sectors of PA and HGL-DTGs defence metabolites, suggesting that herbivore defence responses are amplified in neighbouring plants connected to previously attacked plants via a CMNs. These results indicate that the CMNs among *N. attenuata* plants not only transfer defence signals between herbivore-challenged and unattacked neighbouring plants but also filter both the transmitted signals and the responses activated by these signals. In the following, we discuss the inconsistencies in the literature about these AMF-mediated metabolic responses, alternative interpretation of the data we observed, and the functional interpretations of these responses.

Increased constitutive levels of jasmonates have been reported in mycorrhizal roots of several plant species including *Cucumis sativus* (cucumber; Vierheilig & Piche, 2002), *M. truncatula* (Stumpe et al., 2005), *Glycine max* (Meixner et al., 2005), and *S. lycopersicum* (Rivero, Gamir, Aroca, Pozo, & Flors, 2015). The increases in root jasmonates we report here in *N. attenuata* plants after mycorrhizal colonization (Figure 1) appear to contradict the results from Riedel et al. (2008), which found no changes in root jasmonate levels of rosette-stage *N. attenuata* plants. This apparent contradiction was resolved by the kinetic analysis reported here, where under the same growth condition and AMF taxa, no changes in jasmonate levels were observed when plants were in the rosette-stage of growth but when plants started flowering at 5 wpi, root JA, and JA-Ile significantly increased relative to AMF-free plants (Figure 2a). Similarly, late-stage increases were reported in *Medicago* species at 5 wpi with *R. irregularis* inoculations (Stumpe et al., 2005); here, we detected statistically nonsignificant ($p = .08$) increases, which may be due to our low replication number ($n = 4$; Figure 1) or unknown differences in the growing conditions. The decreased rosette diameters and retarded plant height (Figure 3c) together with locally increased contents of defence compounds (Figures 1 and S1) are consistent with the likely large carbon demands of AMF associations as well as with potential trade-offs between defence and growth (Züst & Agrawal, 2017); hence, the observed reduction in plant growth could also in part result from increases in root defences resulting from the AMF associations (Figures 1 and 3c).

In contrast to these “local” effects in AMF-inoculated roots, systemic effects on leaf jasmonate levels were not observed here in *N. attenuata* (Figure 1), as has been reported from other species such as *Plantago* and *Medicago* (Schweiger, Baier, Persicke, & Muller, 2014). The observation is that the OS-elicited bursts in AMF-associated plants, did not differ significantly from those of AMF-free plants, and is inconsistent with the work in tomato (Song et al., 2013), which reported that herbivore infestation by *Helicoverpa armigera* larvae amplified increases in defence-related gene expression such as *SILOXD*, *SIAOC*, and *SIPI* in *F. mosseae*-associating plants. These apparently contradictory results suggest that these AMF-mediated responses are dependent on the taxa involved in the interaction, as

has been reported for the AMF-mediated drought responses of tomato that differ when plants associate with different AMF inocula (Chitarra et al., 2016). However, they could also reflect the frequent disconnect between transcriptional and metabolic responses that often occur in responses to herbivore attack and highlight one of the advances of this work, where we focused on metabolic responses.

The design of our mesocosm was inspired by the work of Babikova et al. (2013) in which the four plants of a mesocosm are separated by fine mesh. Both designs suffer from potential artefacts that could result from the mechanical disruption of the CMNs among plants in a mesocosm; for future work, we plan to replace the mesh and the use of mechanical disruption with a genetic approach, focusing on silencing the expression of a calcium- and calmodulin-dependent protein kinase (irCCaMK), known to be abrogated in the AMF-colonization process (Groten et al., 2015; Miller et al., 2013; Oldroyd & Downie, 2006; Singh & Parniske, 2012). Another challenge of the mesocosm approach is the difficulty of quantifying root colonization of intact mesocosms and the need to destructively harvest mesocosms to evaluate the AMF colonization rates by microscopic examinations. Here, we took advantage of AMF-indicative blumenol leaf markers (Wang, Schäfer, et al., 2018) and measured the contents of hydroxyblumenol C-glucoside in leaves to obtain an overview of root colonization of all plants at different time points of the experiment and selected mesocosms, which had similar root AMF colonization rates. This analysis also provided key parameters for the *N. attenuata* system such as the intensity of root colonization required to establish a sufficiently strong CMN (hydroxyblumenol C-glucoside, about 100 ng/g FW relative to d_6 -ABA; Figure 3g) to deliver signals among plants by hyphae as well as the time (6 hr in Figure 4a) required to prime “receiver” plants after the OS elicitation of “donor” plants. These results will facilitate the up-coming tests of the phenomena under “real-world” conditions in the field.

The most exciting result of this work was the clearly increased levels of the W + OS-elicited JA and JA-Ile bursts and their associated defence responses observed in CMNs-connected “receiver” plants of group T of the mesocosm experiment (Figures 4 and S2). This mesocosm experiment was designed to control for a number of factors, which have bedevilled previous attempts to examine interplant transmission of defence signalling mediated by AMF networks. By choosing the OS-elicited JA-mediated defences of the *N. attenuata* system, we were able to build on the large knowledge base of prior information available in this system (Groten et al., 2015; Wang, Wilde, et al., 2018) and germane to this discussion, the ability to exclude interplants defence signalling mediated by plant volatiles (Paschold et al., 2006). In the *N. attenuata* system, it is well established that plant size, growth stage, and tissues influence both constitutive and inducible JA-mediated defences (Baldwin, Schmelz, & Ohnmeiss, 1994; Stitz, Gase, Baldwin, & Gaquerel, 2011; Stitz, Hartl, Baldwin, & Gaquerel, 2014; Stork, Diezel, Halitschke, Galis, & Baldwin, 2009) and that AMF associations influence plant size (Riedel et al., 2008; Wang, Wilde, et al., 2018); hence, it was critical to compare W + OS-elicited response in the same tissues from plants that were of the same size and developmental stage. To this end, we designed

the mesocosms to contain four different groups (Figure 3a) that included controls in which plants of a mesocosm had shared a CMN association up until 7 days before the W + OS elicitation of the “donors,” when the AMF network linking the four plants of each mesocosm was removed. These controls insured that the responses of plants at the same stage and size were being compared.

Although the experiment successfully controlled for size and tissue-specific and volatile-associated artefacts, alternative explanations for the apparent AMF mediation of the observed amplifications of the JA bursts need to be considered. The mesh used to separate roots and allow hyphal penetration was not water proof, and hence, water-born OS-elicited signals could have traversed the “nurse plant space” from “donor” plants to amplify the responses in “receiver” plants, except those of Con2, where this space was emptied of soil before OS elicitation of the “donors.” Although it is unlikely that a water-born signal could have diffused across this 4.5-cm-wide “nurse plant” space in 6 hr, we cannot rule out this possibility for the plants of the other three mesocosm groups.

No significant differences in basal jasmonate levels were observed in the unelicited “receiver 3” plants (Figure 4b), which were slightly better connected to the AMF network, as revealed by the foliar hydroxyblumenol C-glucosides contents, than were the receiver 2 plants (Figure 3g), indicating that there were no constitutive changes in jasmonate signalling. The 1.5-fold amplifications of the OS-elicited JA and JA-Ile bursts observed in the “receiver 2” plants of the group T treatment of the mesocosm experiment corresponded nicely with the similar (1.3-fold) increases in JA-associated AA (Figures 4b and 5). Interestingly, the well-described inactivation steps in jasmonate signalling, which includes the oxidation of JA-Ile to OH-JA-Ile and COOH-JA-Ile and the conjugation of JA with valine to form JA-Val (Caarls et al., 2017; Stitz, Baldwin, & Gaquerel, 2011), did not differ among the four groups (Figure S3). In *N. attenuata*, these inactivated forms peak 2 hr after W + OS elicitation and hence represent a metabolically slower step than the accumulation of the active forms such as JA-Ile, which normally peak within 1 hr (Stitz, Gase, et al., 2011). IAA and ABA are additional OS-elicited phytohormones involved in herbivore resistance in *N. attenuata* (Dinh et al., 2013; Hettenhausen et al., 2013; Machado et al., 2016), but their OS-elicited increases were not specifically amplified in mesocosm group T plants and did not vary within 0.5-hr OS elicitation (Figure 4b). Previous studies reported that IAA elicitation occurs very rapidly, within 5 min (Machado et al., 2016), and the 0.5-hr sampling window may have missed the peaking time of this phytohormone. Given the complicated kinetics of many of the W + OS-elicited changes, future work on these AMF-transmitted responses will require a much higher degree of replication in order to capture these different dynamics in destructive harvests.

The second tantalizing result from the mesocosm experiment was that the W + OS-elicited amplification only influenced particular sectors of the metabolic responses known to be OS-elicited by jasmonate signalling in *N. attenuata*. Nicotine, rutin, and CGA are all known to be constitutively expressed and not increased by W + OS elicitation when plants have entered the flowering stage of growth; in contrast, most phenolamides are known to be highly OS-inducible (Gaquerel,

Gulati, & Baldwin, 2014; Kaur, Heinzl, Schottner, Baldwin, & Galis, 2010; Li et al., 2017; Lou & Baldwin, 2003; Ohnmeiss & Baldwin, 2000; Onkokesung et al., 2012). Surprisingly, although the levels of all phenolamides were W + OS induced, the increases were highly variable among the four treatment groups (Figure 6). The relatively larger increases in CP isomers in the Con2 mesocosm group, most likely resulted from priming by inadvertent damage prior to the OS elicitations when the nurse-plant space was emptied (Figure 6). The significantly larger increases in nonmalonylated versions of HGL-DTGs (Figures 7b and S4 and Table S1) in mesocosm group T are particularly noteworthy, suggesting that these particular sectors of DTG metabolism should be more carefully scrutinized for potential functional specificity. At this stage, we can only guess why these particular sectors were amplified by the W + OS elicitation of donor plants connected to receiver plants through the mycorrhizal network and suggest that the mycorrhizal network appears to be able to filter both the signals transmitted by the network and the responses activated by these signals.

5 | CONCLUSION AND FUTURE OUTLOOK

This work demonstrates that mycorrhizal colonization itself does not induce jasmonate-mediated systemic defence responses in leaves of *N. attenuata* plants, whereas systemic defence in leaves can be primed via the belowground CMN to increase antiherbivore defence in neighbouring plants. Whether these AMF network-mediated induced changes increase the resistance of communities of AMF-connected plants and whether the phenomena occurs in the “real world” are important unanswered questions that deserve additional work.

ACKNOWLEDGMENTS

We are grateful to Julia Cramer and Daniel Veit for the mesocosm and irrigation system design. We thank Jiancai Li, Dechang Cao, Suhua Li, and Huili Qiao for help with sampling; Rayko Halitschke, Meredith Schuman, and Ran Li for fruitful discussions; Prof. Maria Harrison for kindly providing *M. truncatula* and *B. distachyon* materials; and reviewers for suggestions and comments. This study was funded by the Max Planck Society, the European Research Council advanced grant ClockworkGreen (No. 293926) to I.T.B. Y.S.'s stay at the MPICoE was funded by China Scholarship Council (# 201608350018) and National Natural Science Foundation of China (31670414 and 31770474).

CONFLICT OF INTEREST

The authors have no conflict of interest to declare.

AUTHOR CONTRIBUTIONS

MW, ITB, YS, and KG planned and designed the research; YS and MW performed the research and analysed the data; ITB and MW wrote the manuscript, with contributions from YS and RZ.

ORCID

Rensen Zeng  <https://orcid.org/0000-0002-6435-3054>

Ian T. Baldwin  <https://orcid.org/0000-0001-5371-2974>

REFERENCES

- Babikova, Z., Gilbert, L., Bruce, T. J., Birkett, M., Caulfield, J. C., Woodcock, C., ... Johnson, D. (2013). Underground signals carried through common mycelial networks warn neighbouring plants of aphid attack. *Ecology Letters*, *16*, 835–843. <https://doi.org/10.1111/ele.12115>
- Bahuliker, R. A., Stanculescu, D., Preston, C. A., & Baldwin, I. T. (2004). ISSR and AFLP analysis of the temporal and spatial population structure of the post-fire annual, *Nicotiana attenuata*, in SW Utah. *BMC Ecology*, *4*, 12–24. <https://doi.org/10.1186/1472-6785-4-12>
- Baldwin, I. T., & Karb, M. J. (1995). Plasticity in allocation of nicotine to reproductive parts in *Nicotiana attenuata*. *Journal of Chemical Ecology*, *21*, 897–909. <https://doi.org/10.1007/BF02033797>
- Baldwin, I. T., Schmelz, E. A., & Ohnmeiss, T. E. (1994). Wound-induced changes in root and shoot jasmonic acid pools correlate with induced nicotine synthesis in *Nicotiana sylvestris* spegazzini and comes. *Journal of Chemical Ecology*, *20*, 2139–2157. <https://doi.org/10.1007/BF02066250>
- Bazzaz, F. (1996). *Plants in changing environments: Linking physiological, population, and community ecology*. Cambridge, UK: Cambridge University press.
- Brundrett, M., Piche, Y., & Peterson, R. (1984). A new method for observing the morphology of vesicular–arbuscular mycorrhizae. *Canadian Journal of Botany*, *62*, 2128–2134. <https://doi.org/10.1139/b84-290>
- Caarls, L., Elberse, J., Awwanah, M., Ludwig, N. R., de Vries, M., Zeilmaker, T., Van Wees, S. C. M., Schuurink, R. C., & Van den, A. G. (2017). Arabidopsis JASMONATE-INDUCED OXYGENASES down-regulate plant immunity by hydroxylation and inactivation of the hormone jasmonic acid. *Proceedings of the National Academy of Sciences of the United States of America*, *114*, 6388–6393.
- Cameron, D. D., Neal, A. L., van Wees, S. C. M., & Ton, J. (2013). Mycorrhiza-induced resistance: More than the sum of its parts? *Trends in Plant Science*, *18*, 539–545. <https://doi.org/10.1016/j.tplants.2013.06.004>
- Cavagnaro, T. R., Bender, S. F., Asghari, H. R., & van der Heijden, M. G. A. (2015). The role of arbuscular mycorrhizas in reducing soil nutrient loss. *Trends in Plant Science*, *20*, 283–290. <https://doi.org/10.1016/j.tplants.2015.03.004>
- Chandanie, W. A., Kubota, M., & Hyakumachi, M. (2006). Interactions between plant growth promoting fungi and arbuscular mycorrhizal fungus *Glomus mosseae* and induction of systemic resistance to anthracnose disease in cucumber. *Plant and Soil*, *286*, 209–217. <https://doi.org/10.1007/s11104-006-9038-y>
- Chitarra, W., Pagliarani, C., Maserti, B., Lumini, E., Siciliano, I., Cascone, P., ... Guerrieri, E. (2016). Insights on the impact of arbuscular mycorrhizal symbiosis on tomato tolerance to water stress. *Plant Physiology*, *171*, 1009–1023. <https://doi.org/10.1104/pp.16.00307>
- Cruz, C., Egsgaard, H., Trujillo, C., Ambus, P., Requena, N., Martins-Loucao, M. A., & Jakobsen, I. (2007). Enzymatic evidence for the key role of arginine in nitrogen translocation by arbuscular mycorrhizal fungi. *Plant Physiology*, *144*, 782–792. <https://doi.org/10.1104/pp.106.090522>
- Currie, A. F., Murray, P. J., & Gange, A. C. (2011). Is a specialist root-feeding insect affected by arbuscular mycorrhizal fungi? *Applied Soil Ecology*, *47*, 77–83. <https://doi.org/10.1016/j.apsoil.2010.12.002>
- De La Noval, B., Pérez, E., Martínez, B., León, O., Martínez-Gallardo, N., & Délano-Frier, J. (2007). Exogenous systemin has a contrasting effect on disease resistance in mycorrhizal tomato (*Solanum lycopersicum*) plants

- infected with necrotrophic or hemibiotrophic pathogens. *Mycorrhiza*, 17, 449–460. <https://doi.org/10.1007/s00572-007-0122-9>
- Dinh, S. T., Baldwin, I. T., & Galis, I. (2013). The HERBIVORE ELICITOR-REGULATED1 gene enhances abscisic acid levels and defenses against herbivores in *Nicotiana attenuata* plants. *Plant Physiology*, 162, 2106–2124. <https://doi.org/10.1104/pp.113.221150>
- Elsen, A., Gervacio, D., Swennen, R., & De Waele, D. (2008). AMF-induced biocontrol against plant parasitic nematodes in *Musa* sp.: A systemic effect. *Mycorrhiza*, 18, 251–256. <https://doi.org/10.1007/s00572-008-0173-6>
- Ezawa, T., Smith, S. E., & Smith, F. A. (2002). P metabolism and transport in AM fungi. *Plant and Soil*, 244, 221–230. <https://doi.org/10.1023/A:1020258325010>
- Fritz, M., Jakobsen, I., Lyngkjær, M. F., Thordal-Christensen, H., & Pons-Kühnemann, J. (2006). Arbuscular mycorrhiza reduces susceptibility of tomato to *Alternaria solani*. *Mycorrhiza*, 16, 413–419. <https://doi.org/10.1007/s00572-006-0051-z>
- Gange, A. C. (2001). Species-specific responses of a root- and shoot-feeding insect to arbuscular mycorrhizal colonization of its host plant. *New Phytologist*, 150, 611–618. <https://doi.org/10.1046/j.1469-8137.2001.00137.x>
- Gange, A. C., Brown, V. K., & Sinclair, G. S. (1994). Reduction of black vine weevil larval growth by vesicular-arbuscular mycorrhizal infection. *Entomologia Experimentalis et Applicata*, 70, 115–119. <https://doi.org/10.1111/j.1570-7458.1994.tb00739.x>
- Gaquerel, E., Gulati, J., & Baldwin, I. T. (2014). Revealing insect herbivory-induced phenolamide metabolism: From single genes to metabolic network plasticity analysis. *Plant Journal*, 79, 679–692. <https://doi.org/10.1111/tpj.12503>
- Giri, B., Kapoor, R., & Mukerji, K. (2003). Influence of arbuscular mycorrhizal fungi and salinity on growth, biomass, and mineral nutrition of *Acacia auriculiformis*. *Biology and Fertility of Soils*, 38, 170–175. <https://doi.org/10.1007/s00374-003-0636-z>
- Govindarajulu, M., Pfeffer, P. E., Jin, H. R., Abubaker, J., Douds, D. D., Allen, J. W., ... Shachar-Hill, Y. (2005). Nitrogen transfer in the arbuscular mycorrhizal symbiosis. *Nature*, 435, 819–823. <https://doi.org/10.1038/nature03610>
- Groten, K., Nawaz, A., Nguyen, N. H. T., Santhanam, R., & Baldwin, I. T. (2015). Silencing a key gene of the common symbiosis pathway in *Nicotiana attenuata* specifically impairs arbuscular mycorrhizal infection without influencing the root-associated microbiome or plant growth. *Plant, Cell & Environment*, 38, 2398–2416. <https://doi.org/10.1111/pce.12561>
- Halitschke, R., Gase, K., Hui, D. Q., Schmidt, D. D., & Baldwin, I. T. (2003). Molecular interactions between the specialist herbivore *Manduca sexta* (Lepidoptera, Sphingidae) and its natural host *Nicotiana attenuata*. VI. Microarray analysis reveals that most herbivore-specific transcriptional changes are mediated by fatty acid-amino acid conjugates. *Plant Physiology*, 131, 1894–1902.
- Heiling, S., Schuman, M. C., Schoettner, M., Mukerjee, P., Berger, B., Schneider, B., ... Baldwin, I. T. (2010). Jasmonate and ppHsystemin regulate key malonylation steps in the biosynthesis of 17-hydroxygeranylinalool diterpene glycosides, an abundant and effective direct defense against herbivores in *Nicotiana attenuata*. *Plant Cell*, 22, 273–292. <https://doi.org/10.1105/tpc.109.071449>
- Hettenhausen, C., Baldwin, I. T., & Wu, J. Q. (2013). *Nicotiana attenuata* MPK4 suppresses a novel jasmonic acid (JA) signaling-independent defense pathway against the specialist insect *Manduca sexta*, but is not required for the resistance to the generalist *Spodoptera littoralis*. *New Phytologist*, 199, 787–799. <https://doi.org/10.1111/nph.12312>
- Hijikata, N., Murase, M., Tani, C., Ohtomo, R., Osaki, M., & Ezawa, T. (2010). Polyphosphate has a central role in the rapid and massive accumulation of phosphorus in extraradical mycelium of an arbuscular mycorrhizal fungus. *New Phytologist*, 186, 285–289. <https://doi.org/10.1111/j.1469-8137.2009.03168.x>
- Hildebrandt, U., Regvar, M., & Bothe, H. (2007). Arbuscular mycorrhiza and heavy metal tolerance. *Phytochemistry*, 68, 139–146. <https://doi.org/10.1016/j.phytochem.2006.09.023>
- Jaiti, F., Meddich, A., & El Hadrami, I. (2007). Effectiveness of arbuscular mycorrhizal fungi in the protection of date palm (*Phoenix dactylifera* L.) against bayoud disease. *Physiological and Molecular Plant Pathology*, 71, 166–173. <https://doi.org/10.1016/j.pmp.2008.01.002>
- Howe, G. A., & Jander, G. (2008). Plant immunity to insect herbivores. *Annual Review of Plant Biology*, 59, 41–66.
- Javot, H., Penmetsa, R. V., Terzaghi, N., Cook, D. R., & Harrison, M. J. (2007). A *Medicago truncatula* phosphate transporter indispensable for the arbuscular mycorrhizal symbiosis. *Proceedings of the National Academy of Sciences of the United States of America*, 104, 1720–1725.
- Johnson, N. C., Graham, J. H., & Smith, F. A. (1997). Functioning of mycorrhizal associations along the mutualism-parasitism continuum. *New Phytologist*, 135, 575–586. <https://doi.org/10.1046/j.1469-8137.1997.00729.x>
- Jung, S. C., Martinez-Medina, A., Lopez-Raez, J. A., & Pozo, M. J. (2012). Mycorrhiza-induced resistance and priming of plant defenses. *Journal of Chemical Ecology*, 38, 651–664. <https://doi.org/10.1007/s10886-012-0134-6>
- Kaur, H., Heinzel, N., Schottner, M., Baldwin, I. T., & Galis, I. (2010). R2R3-NaMYB8 Regulates the accumulation of phenylpropanoid-polyamine conjugates, which are essential for local and systemic defense against insect herbivores in *Nicotiana attenuata*. *Plant Physiology*, 152, 1731–1747. <https://doi.org/10.1104/pp.109.151738>
- Krugel, T., Lim, M., Gase, K., Halitschke, R., & Baldwin, I. T. (2002). Agrobacterium-mediated transformation of *Nicotiana attenuata*, a model ecological expression system. *Chemoecology*, 12, 177–183. <https://doi.org/10.1007/PL00012666>
- Laparré, J., Malbreil, M., Letisse, F., Portais, J. C., Roux, C., Becard, G., & Puech-Pages, V. (2014). Combining metabolomics and gene expression analysis reveals that propionyl- and butyryl-carnitines are involved in late stages of arbuscular mycorrhizal symbiosis. *Molecular Plant*, 7, 554–566. <https://doi.org/10.1093/mp/sst136>
- Lee, C. S., Lee, Y. J., & Jeun, Y. C. (2005). Observations of infection structures on the leaves of cucumber plants pre-treated with arbuscular mycorrhiza *Glomus intraradices* after challenge inoculation with *Colletotrichum orbiculare*. *Plant Pathology Journal*, 21, 237–243. <https://doi.org/10.5423/PPJ.2005.21.3.237>
- Lee, G., Joo, Y., Kim, S. G., & Baldwin, I. T. (2017). What happens in the pith stays in the pith: Tissue-localized defense responses facilitate chemical niche differentiation between two spatially separated herbivores. *Plant Journal*, 92, 414–425. <https://doi.org/10.1111/tpj.13663>
- Lenoir, I., Fontaine, J., & Sahaoui, A. L. H. (2016). Arbuscular mycorrhizal fungal responses to abiotic stresses: A review. *Phytochemistry*, 123, 4–15. <https://doi.org/10.1016/j.phytochem.2016.01.002>
- Li, R., Wang, M., Wang, Y., Schuman, M. C., Weinhold, A., Schafer, M., Jimenez-Aleman, G. H., Barthel, A., & Baldwin, I. T. (2017). Flower-specific jasmonate signaling regulates constitutive floral defenses in wild tobacco. *Proceedings of the National Academy of Sciences of the United States of America*, 114, E7205–7214.
- Lopez-Raez, J. A., Pozo, M. J., & Garcia-Garrido, J. M. (2011). Strigolactones: a cry for help in the rhizosphere. *Botany-Botanique*, 89, 513–522. <https://doi.org/10.1139/b11-046>

- Lou, Y., & Baldwin, I. T. (2003). Manduca sexta recognition and resistance among allopolyploid *Nicotiana* host plants. *Proceedings of the National Academy of Sciences of the United States of America*, 100, 14581–14586.
- Luginbuehl, L. H., & Oldroyd, G. E. D. (2017). Understanding the arbuscule at the heart of endomycorrhizal symbioses in plants. *Current Biology*, 27, R952–R963. <https://doi.org/10.1016/j.cub.2017.06.042>
- Machado, R. A. R., Robert, C. A. M., Arce, C. C. M., Ferrieri, A. P., Xu, S. Q., Jimenez-Aleman, G. H., ... Erb, M. (2016). Auxin is rapidly induced by herbivore attack and regulates a subset of systemic, jasmonate-dependent defenses. *Plant Physiology*, 172, 521–532. <https://doi.org/10.1104/pp.16.00940>
- MacLean, A. M., Bravo, A., & Harrison, M. J. (2017). Plant signaling and metabolic pathways enabling arbuscular mycorrhizal symbiosis. *Plant Cell*, 29, 2319–2335. <https://doi.org/10.1105/tpc.17.00555>
- Martin, F. M., Uroz, S., & Barker, D. G. (2017). Ancestral alliances: Plant mutualistic symbioses with fungi and bacteria. *Science*, 356(6340), eaad4501. <https://doi.org/10.1126/science.aad4501>
- Meixner, C., Ludwig-Muller, J., Miersch, O., Gresshoff, P., Staehelin, C., & Vierheilig, H. (2005). Lack of mycorrhizal autoregulation and phytohormonal changes in the supernodulating soybean mutant *nts1007*. *Planta*, 222, 709–715. <https://doi.org/10.1007/s00425-005-0003-4>
- Miller, J. B., Pratap, A., Miyahara, A., Zhou, L., Bornemann, S., Morris, R. J., & Oldroyd, G. E. D. (2013). Calcium/calmodulin-dependent protein kinase is negatively and positively regulated by calcium, providing a mechanism for decoding calcium responses during symbiosis signaling. *Plant Cell*, 25, 5053–5066. <https://doi.org/10.1105/tpc.113.116921>
- Mindt, E., Wang, M., Schäfer, M., Halitschke, R., & Baldwin, I. T. (2019). Quantification of Blumenol Derivatives as Leaf Biomarkers for Plant-AMF Association. *Bio-protocol*, 9(14), e3301. <https://doi.org/10.21769/BioProtoc.3301>
- Møller, K., Kristensen, K., Yohalem, D., & Larsen, J. (2009). Biological management of gray mold in pot roses by co-inoculation of the biocontrol agent *Ulocladium atrum* and the mycorrhizal fungus *Glomus mosseae*. *Biological Control*, 49, 120–125. <https://doi.org/10.1016/j.biocontrol.2009.01.015>
- Ohnmeiss, T. E., & Baldwin, I. T. (2000). Optimal Defense theory predicts the ontogeny of an induced nicotine defense. *Ecology*, 81, 1765–1783. [https://doi.org/10.1890/0012-9658\(2000\)081\[1765:ODPTPO\]2.0.CO;2](https://doi.org/10.1890/0012-9658(2000)081[1765:ODPTPO]2.0.CO;2)
- Oldroyd, G. E. D., & Downie, J. A. (2006). Nuclear calcium changes at the core of symbiosis signalling. *Current Opinion in Plant Biology*, 9, 351–357. <https://doi.org/10.1016/j.pbi.2006.05.003>
- Onkokesung, N., Gaquerel, E., Kotkar, H., Kaur, H., Baldwin, I. T., & Galis, I. (2012). MYB8 controls inducible phenolamide levels by activating three novel hydroxycinnamoyl-coenzyme a: Polyamine transferases in *Nicotiana attenuata*. *Plant Physiology*, 158, 389–407. <https://doi.org/10.1104/pp.111.187229>
- Paschold, A., Halitschke, R., & Baldwin, I. T. (2006). Using 'mute' plants to translate volatile signals. *Plant Journal*, 45, 275–291. <https://doi.org/10.1111/j.1365-313X.2005.02623.x>
- Perry, D. A. (1995). Self-organizing systems across scales. *Trends in Ecology & Evolution*, 19, 241–244.
- Pineda, A., Zheng, S. J., Van Loon, J. J., Pieterse, C. M., & Dicke, M. (2010). Helping plants to deal with insects: The role of beneficial soil-borne microbes. *Trends in Plant Science*, 15, 507–514. <https://doi.org/10.1016/j.tplants.2010.05.007>
- Pozo, M. J., Jung, S. C., López-Ráez, J. A., & Azcón-Aguilar, C. (2010). Impact of arbuscular mycorrhizal symbiosis on plant response to biotic stress: The role of plant defence mechanisms. In *Arbuscular mycorrhizas: physiology and function* (pp. 193–207). Dordrecht: Springer.
- Riedel, T., Groten, K., & Baldwin, I. T. (2008). Symbiosis between *Nicotiana attenuata* and *Glomus intraradices*: Ethylene plays a role, jasmonic acid does not. *Plant, Cell & Environment*, 31, 1203–1213. <https://doi.org/10.1111/j.1365-3040.2008.01827.x>
- Rivero, J., Gamir, J., Aroca, R., Pozo, M. J., & Flors, V. (2015). Metabolic transition in mycorrhizal tomato roots. *Frontiers in Microbiology*, 6, 598.
- Rodríguez, R. J., Henson, J., Van Volkenburgh, E., Hoy, M., Wright, L., Beckwith, F., ... Redman, R. S. (2008). Stress tolerance in plants via habitat-adapted symbiosis. *ISME Journal*, 2, 404–416. <https://doi.org/10.1038/ismej.2007.106>
- Schäfer, M., Brütting, C., Baldwin, I. T., & Kallenbach, M. (2016). High-throughput quantification of more than 100 primary-and secondary-metabolites, and phytohormones by a single solid-phase extraction based sample preparation with analysis by UHPLC–HESI–MS/MS. *Plant Methods*, 12, 30. <https://doi.org/10.1186/s13007-016-0130-x>
- Schausberger, P., Peneder, S., Jurschik, S., & Hoffmann, D. (2012). Mycorrhiza changes plant volatiles to attract spider mite enemies. *Functional Ecology*, 26, 441–449. <https://doi.org/10.1111/j.1365-2435.2011.01947.x>
- Schuman, M. C., & Baldwin, I. T. (2016). The layers of plant responses to insect herbivores. *Annual Review of Entomology*, 61, 373–394. <https://doi.org/10.1146/annurev-ento-010715-023851>
- Schussler, A., Schwarzott, D., & Walker, C. (2001). A new fungal phylum, the Glomeromycota: Phylogeny and evolution. *Mycological Research*, 105, 1413–1421. <https://doi.org/10.1017/S0953756201005196>
- Schweiger, R., Baier, M. C., Persicke, M., & Müller, C. (2014). High specificity in plant leaf metabolic responses to arbuscular mycorrhiza. *Nature Communications*, 5, 3886. <https://doi.org/10.1038/ncomms4886>
- Selosse, M. A., Richard, F., He, X., & Simard, S. W. (2006). Mycorrhizal networks: des liaisons dangereuses? *Trends in Ecology & Evolution*, 21, 621–628. <https://doi.org/10.1016/j.tree.2006.07.003>
- Simard, S. W., Beiler, K. J., Bingham, M. A., Deslippe, J. R., Philip, L. J., & Teste, F. P. (2012). Mycorrhizal networks: Mechanisms, ecology and modelling. *Fungal Biology Reviews*, 26, 39–60. <https://doi.org/10.1016/j.fbr.2012.01.001>
- Singh, S., & Parniske, M. (2012). Activation of calcium-and calmodulin-dependent protein kinase (CCaMK), the central regulator of plant root endosymbiosis. *Current Opinion in Plant Biology*, 15, 444–453. <https://doi.org/10.1016/j.pbi.2012.04.002>
- Smith, S. E., & Read, D. J. (2010). *Mycorrhizal symbiosis*. London, UK: Academic press.
- Song, Y. Y., Ye, M., Li, C. Y., Wang, R. L., Wei, X. C., Luo, S. M., & Zeng, R. S. (2013). Priming of anti-herbivore defense in tomato by arbuscular mycorrhizal fungus and involvement of the jasmonate pathway. *Journal of Chemical Ecology*, 39, 1036–1044. <https://doi.org/10.1007/s10886-013-0312-1>
- Stitz, M., Baldwin, I. T., & Gaquerel, E. (2011). Diverting the flux of the JA pathway in *Nicotiana attenuata* compromises the plant's defense metabolism and fitness in nature and glasshouse. *PLoS ONE*, 6(10), e25925. <https://doi.org/10.1371/journal.pone.0025925>
- Stitz, M., Gase, K., Baldwin, I. T., & Gaquerel, E. (2011). Ectopic expression of AtJMT in *Nicotiana attenuata*: Creating a metabolic sink has tissue-specific consequences for the jasmonate metabolic network and silences downstream gene expression. *Plant Physiology*, 157, 341–354. <https://doi.org/10.1104/pp.111.178582>
- Stitz, M., Hartl, M., Baldwin, I. T., & Gaquerel, E. (2014). Jasmonoyl-L-isoleucine coordinates metabolic networks required for anthesis and floral attractant emission in wild tobacco (*Nicotiana attenuata*). *Plant Cell*, 26, 3964–3983. <https://doi.org/10.1105/tpc.114.128165>

- Stork, W., Diezel, C., Halitschke, R., Galis, I., & Baldwin, I. T. (2009). An ecological analysis of the herbivory-elicited JA burst and its metabolism: Plant memory processes and predictions of the moving target model. *PLoS ONE*, 4(3). <https://doi.org/10.1371/journal.pone.0004697>
- Stumpe, M., Carsjens, J. G., Stenzel, I., Gobel, C., Lang, I., Pawlowski, K., ... Feussner, I. (2005). Lipid metabolism in arbuscular mycorrhizal roots of *Medicago truncatula*. *Phytochemistry*, 66, 781–791. <https://doi.org/10.1016/j.phytochem.2005.01.020>
- Tanaka, Y., & Yano, K. (2005). Nitrogen delivery to maize via mycorrhizal hyphae depends on the form of N supplied. *Plant, Cell & Environment*, 28, 1247–1254. <https://doi.org/10.1111/j.1365-3040.2005.01360.x>
- Tanwar, A., Aggarwal, A., & Panwar, V. (2013). Arbuscular mycorrhizal fungi and *Trichoderma viride* mediated Fusarium wilt control in tomato. *Bio-control Science and Technology*, 23, 485–498. <https://doi.org/10.1080/09583157.2013.772561>
- Brundrett, M. C., & Tedersoo, L. (2018). Evolutionary history of mycorrhizal symbioses and global host plant diversity. *New Phytologist*, 220, 1108–1115.
- Van Der Heijden, M. G. A., & Horton, T. R. (2009). Socialism in soil? The importance of mycorrhizal fungal networks for facilitation in natural ecosystems. *Journal of Ecology*, 97, 1139–1150. <https://doi.org/10.1111/j.1365-2745.2009.01570.x>
- Vierheilig, H., & Piche, Y. (2002). Signalling in arbuscular mycorrhiza: Facts and hypotheses. In *Flavonoids in cell function* (pp. 23–39). Boston, MA: Springer.
- Vierheilig, H., Schweiger, P., & Brundrett, M. (2005). An overview of methods for the detection and observation of arbuscular mycorrhizal fungi in roots. *Physiologia Plantarum*, 125, 393–404.
- Vos, C., Claerhout, S., Mkandawire, R., Panis, B., de Waele, D., & Elsen, A. (2012). Arbuscular mycorrhizal fungi reduce root-knot nematode penetration through altered root exudation of their host. *Plant and Soil*, 354, 335–345. <https://doi.org/10.1007/s11104-011-1070-x>
- Wang, M., Schäfer, M., Li, D., Halitschke, R., Dong, C., McGale, E., ... Baldwin, I. T. (2018). Blumenols as shoot markers for root symbiosis with arbuscular mycorrhizal fungi. *eLife*, 7, e37093. <https://doi.org/10.7554/eLife.37093>
- Wang, M., Wilde, J., Baldwin, I. T., & Groten, K. (2018). *Nicotiana attenuata*'s capacity to interact with arbuscular mycorrhiza alters its competitive ability and elicits major changes in the leaf transcriptome. *Journal of Integrative Plant Biology*, 60, 242–261. <https://doi.org/10.1111/jipb.12609>
- Wu, J. Q., & Baldwin, I. T. (2010). New insights into plant responses to the attack from insect herbivores. *Annual Review of Genetics*, 44, 1–24. <https://doi.org/10.1146/annurev-genet-102209-163500>
- Züst, T., & Agrawal, A. A. (2017). Trade-offs between plant growth and defense against insect herbivory: An emerging mechanistic synthesis. *Annual Review of Plant Biology*, 68, 513–534. <https://doi.org/10.1146/annurev-arplant-042916-040856>

SUPPORTING INFORMATION

Additional supporting information may be found online in the Supporting Information section at the end of the article.

Fig. S1 AMF-induced increases in constitutive jasmonates in the roots of *N. attenuata* do not translate into systemic increases in JA-dependent secondary metabolites in leaves

Figure S2 Mesocosm design, mesocosms grouping and experimental procedures.

Figure S3 Evidence of AMF-mediated defense priming: bursts of inactive jasmonate forms are not amplified in the “receiver” plants of the AMF mycelia group (T) after the W + OS elicitation of the “donor” plants. Details are as described in Figure 4.

Figure S4 Hydroxygeranylinalool diterpene glycosides (HGL-DTGs) exhibit compound-specific increases in response to W + OS elicitation among the 4 mesocosm treatment groups.

Table. S1 Numerical values of each HGL-DTG relative concentration and statistical analysis.

Table. S2 Primer sequences for Quantitative (q)PCR.

How to cite this article: Song Y, Wang M, Zeng R, Groten K, Baldwin IT. Priming and filtering of antiherbivore defences among *Nicotiana attenuata* plants connected by mycorrhizal networks. *Plant Cell Environ*. 2019;42:2945–2961. <https://doi.org/10.1111/pce.13626>